Modeling Metal Removal onto Natural Particles Formed during Mixing of Acid Rock Drainage with Ambient Surface Water

JENNIFER W. TONKIN,*,†
LAURIE S. BALISTRIERI,‡,§ AND
JAMES W. MURRAY†,‡

Department of Chemistry, University of Washington, Seattle, Washington 98195-1700, U.S. Geological Survey, Seattle, Washington 98195-7940, and School of Oceanography, University of Washington, Seattle, Washington 98195-7940

Studies have examined partitioning of trace metals onto natural particles to better understand the fate and transport of trace metals in the environment, but few studies have compared model predictions with field results. We evaluate the application of an empirical modeling approach, using surface complexation parameters available in the literature, to complex natural systems. In this work, the equilibrium speciation computer program PHREEQC was used along with the diffuse double-layer surface complexation model to simulate metal removal onto natural oxide particles formed during the mixing of acid rock drainage with ambient surface water. End-member solutions sampled in the Coeur d'Alene (CdA) Mining District in September 1999 from the Bunker Hill Mine and the South Fork Coeur d'Alene (SFCdA) River were filtered and mixed in several ratios. Solution chemistry was determined for end-members and mixed solutions, and X-ray diffraction (XRD) was used to determine the mineralogy of precipitate phases. Predicted amounts of Fe precipitates were in good agreement with measured values for particulate Fe. Surface area and reactive site characteristics were used along with surface complexation constants for ferrihydrite (Dzombak, D. A.; Morel, F. M. M. *Surface Complexation Modeling: Hydrous Ferric Oxide*; John Wiley & Sons: New York, 1990) to predict ion sorption as a function of mixing fraction. Comparisons of model predictions with field results indicate that Pb and Cu sorption are predicted well by the model, while As, Mo, and Sb sorption are less well-predicted. Additional comparisons with particulate metal and Fe data collected from the CdA Mining District in 1996 and 1997 suggest that sorption on particulate Fe, including amorphous iron oxides and schwertmannite, may be described using universal model parameters.

Introduction

The geochemical interaction between ambient waters and wastes generated from mining and processing of ore deposits is an important area of study due to potential environmental impacts and health concerns. Exposure of pyrite and other sulfide minerals to natural weathering agents increases the acidity and metal content of waters draining mine deposits, ultimately affecting environmental water quality. Studies have focused on geologic and geochemical controls that affect mine drainage composition and the mobility and attenuation of metals, including precipitation, adsorption onto existing suspended particulates, and adsorption onto newly formed solids (1–5). Acidic waters containing high concentrations of metals, including Fe, Mn, and Al, can mix with near-neutral groundwater and surface water over regions on the scale of kilometers, and geochemical processes can occur that remove metals from solution (6–8). Further investigation of these processes, including the sorption characteristics of newly formed solid phases, will help us better understand the fate and transport of metals upon natural mixing of different water types.

Surface and solution reactions have been paired in a number of surface complexation models (SCMs) to extend the model of metal partitioning over a wide range of solution compositions. Databases for hydrous ferric oxide (HFO) (9), goethite (10), and Al_2O_3 (11) have been developed using laboratory-derived sorption data and the diffuse double-layer SCM with the aim of creating a consistent approach to predictive modeling of metal partitioning onto multiple sorbing phases. Using the available laboratory-based models, predictions of metal partitioning onto oxide phases have been compared with field measurements (12, 13), and recent studies have focused upon the chemical transformations and metal transport and removal processes that occur in the natural mixing zones of areas impacted by acid mine drainage (14–16). Bridging the gap between the laboratory and a complex natural environment requires laboratory-derived sorption data, field measurements, and a critical evaluation of the validity of the modeling approach. There are two possible modeling approaches: use of a universal model, where existing databases are used, or use of a conditional model, where surface characteristics and sorption parameters are determined for each individual site. Using the Coeur d'Alene Mining District as a natural laboratory, we evaluate the ability of the diffuse double-layer SCM, incorporating the databases for iron and aluminum oxides, to predict metal removal onto newly formed natural particles formed during mixing of acid mine drainage with ambient surface water. Additionally, we are able to assess the applicability of the chosen universal approach to systems where solution conditions and complex mineralogy may not be well-characterized.

Study Area

The Coeur d'Alene (CdA) Mining District is located in the Bitterroot Mountains of northern Idaho. The district is traversed by a near-50-km length of the South Fork Coeur d'Alene (SFCdA) River. The district historically ranks as one of the largest producers of Ag in the world, and one of the largest producers of Pb and Zn in the United States. The principal economic minerals are galena (PbS), sphalerite (ZnS), and tetrahedrite [$(Cu,Fe)_{12}Sb_4S_{13}$]. Sphalerite can contain other metals such as Fe, Cu, Cd, and Mn (17). In tetrahedrite, Zn, Ag, Cd, and Hg can substitute for Cu and As, Bi, and Te can substitute for Fe (18). Pyrite is ubiquitous but variable in abundance. Before the requirement of tailings ponds in 1968, mining wastes from over a century of mining, milling, and ore processing were discharged directly to surface waters (19, 20). Today, the SFCdA River is a repository for 72 million tons of mining waste (21). Drainage from adits and tailings piles in the CdA Mining District range from near

* Corresponding author e-mail: jtonkin@u.washington.edu; phone: (206)543-0632; fax: (206) 685-3351.
† Department of Chemistry, University of Washington.
‡ School of Oceanography, University of Washington.
§ U.S. Geological Survey.

neutral to acidic and have highly variable concentrations and compositions of metals, while the SFCdA River is near neutral (*17*).

The Bunker Hill Mine in Kellogg, ID, was once one of the largest Pb and Zn mines in the United States and is now part of the U.S. Environmental Protection Agency's Bunker Hill Superfund site. The 54-km² site in the CdA Mining District is one of the largest abandoned hazardous waste sites in the nation. The sulfidic mineralogy of the Bunker Hill mine is complex and gives rise to a range of metals and metalloids in the acid discharge. Water percolating downward through overlying sulfide-bearing strata is combined with water pumped from lower levels, transported from the mine through the Kellogg Tunnel, and eventually treated (*22*). To study the mixing of different source waters, we chose the SFCdA River and the effluent from the Bunker Hill Mine as end-member solutions representative of the geologic and geochemical characteristics of the CdA Mining District. Contaminated surface water from the SFCdA River was collected in Osburn, upstream or east of the Bunker Hill site, on September 23, 1999; and acid rock drainage from the Bunker Hill Mine was collected from the treatment pond on the Bunker Hill site on September 24, 1999.

Methods

Mixing Experiments. A peristaltic pump, Teflon tubing, and an in-line 0.45 μM cartridge filter were used to collect the end-member solutions into 20-L acid-cleaned, well-rinsed cubitainers that had been rinsed three times with the end-member solution before collection. The Bunker Hill (BH) effluent was stored in the dark to minimize photooxidation reactions.

Small- and large-scale mixing experiments were conducted. Large-scale experiments were conducted to precipitate sufficient solid material for further study. All mixing vessels were acid-cleaned and well-rinsed with distilled deionized water. BH and SFCdA River end-members were mixed immediately after collection of the BH end-member solution in BH:SFCdA ratios of approximately 1:1000, 1:200, 1:40, 1:17, 1:10, 1:5, 1:4, 1:3, and 1:2. For small-scale mixing experiments, CdA River water was added to BH effluent aliquots in 1-L high-density polyethylene (HDPE) bottles. Duplicate small-scale experiments were performed at mixing ratios of approximately 1:5 and 1:17. Kinetic data were collected at intervals of 2.5, 14, 24, and 49 h. Large-scale mixing experiments were performed at mixing ratios of 1:40, 1:17, and 1:5 in 20-L HDPE cubitainers, including one duplicate experiment at the ratio of 1:17. Samples were mixed thoroughly and allowed to stand in the dark for 24 h, with the exception of the kinetic experiments.

Analyses were performed on the SFCdA River and BH end-member solutions and all mixing experiments. Temperature, conductivity, and pH were measured within 24−28 h after oxidation, precipitation, and adsorption reactions had occurred. A 30-mL unfiltered sample was collected in an acid-cleaned HDPE bottle, acidified with 3 drops of redistilled concentrated HNO$_3$, and stored for total acid-soluble metal analysis by ICP-MS, ICP-AES, or AAS. Aliquots of 30, 8, and 30 mL were filtered through a 0.45 μM nylon syringe filter for dissolved metals, alkalinity, and Fe(II) analysis, respectively. The sample for dissolved metals analysis was acidified with 3 drops of redistilled concentrated HNO$_3$ and stored for analysis by ICP-MS, ICP-AES, or AAS. The Fe(II) sample was preserved with 5 drops of redistilled concentrated HCl and stored in a dark bottle. Additional aliquots were filtered through GFF filters and stored unpreserved in HDPE bottles for anion analysis. The volume filtered through each GFF filter was recorded, and the filters were stored for particulate organic carbon (POC) analysis. Precipitates formed during the mixing experiments were kept in the mixed solution and saved for X-ray diffraction (XRD) analysis.

Alkalinity and Fe(II) analyses were performed within 48 h. Alkalinity was determined by Gran titration (*23*), and Fe-(II) was determined colorimetrically by reaction with 1,10-phenanthroline. Metals were determined by ICP-MS except Ca and Mg, which were determined by ICP-AES, and Fe, K, and Na, which were determined by AAS. Concentrations of major anions were determined by ion chromatography. Field and filter blanks, sample duplicates, and reference standards were analyzed with each batch of samples. Blank concentrations were generally below detection limits, and sample concentrations were corrected for measurable blank values. Analyses of duplicate field samples were in good agreement. Measured concentrations were within acceptable error limits for all published reference standard values. XRD analysis of the precipitates was performed using an automated Phillips XRD system using Cu Kα-1 radiation.

Model Simulations. Modeling was performed with the computer program PHREEQC2.2 (*24*). Model simulations considered the formation of solution complexes, precipitation of solid phases, and sorption onto newly formed iron and aluminum oxide phases. The thermodynamic database from MINTEQA2 (*25*) was used to perform equilibrium speciation calculations. Solution and solid-phase reactions for Co, Cs, and Mo (*26*); the formation reaction for schwertmannite [(Fe$_8$O$_8$(OH)$_6$SO$_4$)] (*27*); and surface complexation reactions for HFO (*9*) and Al$_2$O$_3$ (*11*) were added to the database. The effects of the competition of multiple metals for the sorbing surface were evaluated by considering all sorption reactions in a single model simulation.

Model inputs included measured temperature, pH, alkalinity, anions, and dissolved metal measurements for each end-member solution and calculated pE and mixing fraction (Table 1). The pE value for the BH end-member solution was optimized using comparisons of measured dissolved Fe(II) to Fe(III) (calculated by subtracting measured dissolved Fe-(II) from dissolved Fe) ratios to predicted Fe speciation. The pE value for the SFCdA River end-member solution was calculated using the measured pH value and assuming equilibrium with atmospheric O$_2$ (*23*). Because both Fe(II) and Fe(III) measurements of the SFCdA River water were at or close to detection limits, we assumed that all total acid-soluble Fe was present as Fe(III). Mixing fractions were calculated using the concentrations of total acid-soluble Na and assuming conservative mixing of the end-member solutions.

Mixing simulations in PHREEQC were run at each mixing fraction without equilibration of any solids to determine equilibrium phases. The model results indicated that Fe and Al phases and barite (BaSO$_4$) were supersaturated at all mixing fractions. On the basis of these results, all mixed solutions were equilibrated with barite, gibbsite and hydrous ferric oxide (HFO), goethite, or schwertmannite. Additionally, Ba$_3$-(AsO$_4$)$_2$, at mixing ratios of BH to CdA River water $\geq$1:4; birnessite, at mixing ratios of BH to CdA River water >1:5; and otavite (CdCO$_3$), at the highest mixing ratio of 1:17, were found to be supersaturated and were included as equilibrium phases at the corresponding mixing fractions. All mixed solutions were equilibrated with pCO$_2$ = 2.45, calculated from the measured pH and alkalinity of the CdA River end-member solution.

In the model simulations, the site concentration of each sorbing surface was calculated based upon the surface parameters assigned to each corresponding equilibrium phase. HFO surface parameters (*9*) were used for all iron oxide phases, and Al$_2$O$_3$ surface parameters (*11*) were used for gibbsite. Birnessite was included as an equilibrium phase but was not considered in the sorption model. Model parameters for iron oxide phases included a specific surface

	Bunker Hill	South Fork Coeur d'Alene River
temp (°C)	22.1	22.1
pH	2.85	7.36
alkalinity (mequiv L^{-1})	0	1.4
anions (mg L^{-1})		
Cl	1.2	3.0
F	0.1	0.1
NO$_3$	0.6	0.9
SO$_4$	930	24
dissolved metals (μg L^{-1})		
Al	4860	3.8
As	50	0.78
Ba	32	67
Be	1.5	nd[a]
Ca	43 000	21 000
Cd	316	8.9
Co	106	0.11
Cr	1.9	0.12
Cs	0.50	0.20
Cu	275	1.5
Fe	115 000	200
Fe(II)	16 905	16
K	1370	1290
Mg	66 000	6300
Mn	44	0.03
Mo	0.04	0.51
Na	1070	4000
Ni	96	0.85
Pb	413	12
Rb	5.0	2.1
Sb	0.09	4.8
Sr	43	88
Tl	0.19	nd
U	3.2	0.19
Zn	162 300	1070

[a] Not detectable.

TABLE 2. Iron Oxide Equilibrium Phase as a Function of Mixing Fraction Bunker Hill (BH) Effluent

mixing fraction BH	measd pH	equilibrium phase (by XRD) major	minor	trace
0.474	2.9	schwertmannite		
0.467	3.0	schwertmannite	goethite	
0.385	3.1	schwertmannite	goethite	
0.323	3.1	goethite		schwertmannite
0.265	3.3	goethite		schwertmannite
0.241	3.4	goethite		schwertmannite
0.189	3.5	goethite		schwertmannite
0.186	3.8	goethite		schwertmannite
0.182	3.8	goethite		
0.120	6.0	amorphous		schwertmannite
0.086	6.5	amorphous		schwertmannite
0.082	6.4	na[a]		
0.062	6.6	na		
0.062	6.3	amorphous	goethite	

[a] Not analyzed.

area of 600 m^2 g^{-1}, strong site density of 0.005 mol mol Fe^{-1}, and weak site density of 0.2 mol mol Fe^{-1} (9). The weak binding constant for Pb for iron oxide phases was increased from 10$^{0.3}$ to 10$^{1.3}$, consistent with previous modeling studies (16). For gibbsite, model parameters included a specific surface area of 129 m^2 g^{-1}, strong site density of 6.6 × 10^{-4} mol mol Al^{-1}, and weak site density of 5.9 × 10^{-3} mol mol Al^{-1} (11). The surfaces were reacted with the mixed solutions, and the resulting new equilibrium solution and surface species concentrations were used for the subsequent discussion.

Data Analysis. Mass balances were investigated by comparing the mass of each element calculated using the measured end-member values and the mixing fractions with the measured total acid-soluble mass in the mixing experiments. Metal removal was first investigated by plotting the dissolved metal concentrations for the end-member and mixed solutions as a function of the mixing fraction. The metals that showed deviations from the conservative mixing line were considered removed from solution, and particulate metal concentrations were calculated by subtracting measured dissolved metal from total acid-soluble metal values. Conservative behavior of the elements upon end-member solution mixing was assumed when generating error bars for measured particulate metal. Error estimates for measured total acid-soluble, particulate, and dissolved metal values were determined for Fe, Pb, Cu, As, Mo, and Sb by generating a linear plot of measured total acid-soluble metal concentrations as a function of mixing fraction. Standard deviation values determined from the linear regression analyses were used in all subsequent error analyses.

Results and Discussion

We compare model results for the formation of particulate iron and aluminum oxide phases and sorption of metals onto these particles with observed removal during mixing experiments and with metal partitioning in mine drainage waters.

Newly Formed Particles. The XRD data illustrate the variation in structure and crystallinity of the iron oxides formed in situ as a function of pH, which is consistent with observed variations in color and particle size of the precipitates. The solid material analyzed by XRD was found to be mostly amorphous (i.e., without crystalline structure and therefore not matched to a XRD pattern), but some samples showed the presence of crystalline iron oxide phases. Table 2 summarizes the mineralogy of iron oxide phases as a function of the mixing fraction. Schwertmannite was the major phase, and goethite was a minor or trace phase for mixed solutions of pH values 2.9−3.1. Solutions of pH 3.1−5.5 produced predominantly goethite with traces of schwertmannite. Solutions of pH 6.0−6.5 were comprised of major amorphous material with goethite as a minor phase and traces of schwertmannite. Our results are consistent with earlier reports describing the mineralogy of natural precipitates collected from mine drainage waters in Ohio (27). On the basis of these results, amorphous Fe and Al or crystalline iron oxide phases were chosen as the equilibrium solid phases in the mixing simulations using PHREEQC, with the surface characteristics of hydrous ferric oxide (HFO) universally assigned to the sorbing Fe solids. Measured pH values are not linear with mixing fraction, and predicted and measured pH as a function of mixing fraction is shown in Figure 1a. Mixed solutions will be identified hereafter by mixing fraction with the corresponding pH values given as a general reference.

Mass balances were in good agreement within measurement error. Metal removal was significant for Fe and Al, and the amount removed was assumed to represent the sorbent phase characterized by XRD. Predicted particulate Fe in the mixed solutions versus measured particulate Fe is shown in Figure 1b. There is generally good agreement between modeled and measured values within a factor of 1.5 using HFO and the major phases determined by XRD. Model predictions deviate further from measured particulate Fe values when the equilibrium phase used in the model simulations is not matched to the phase determined by XRD. However, these deviations increase with decreasing pH, suggesting that at higher pH values the XRD data may not be so important, in agreement with the amorphous nature of the iron oxide solids formed. However, we recommend
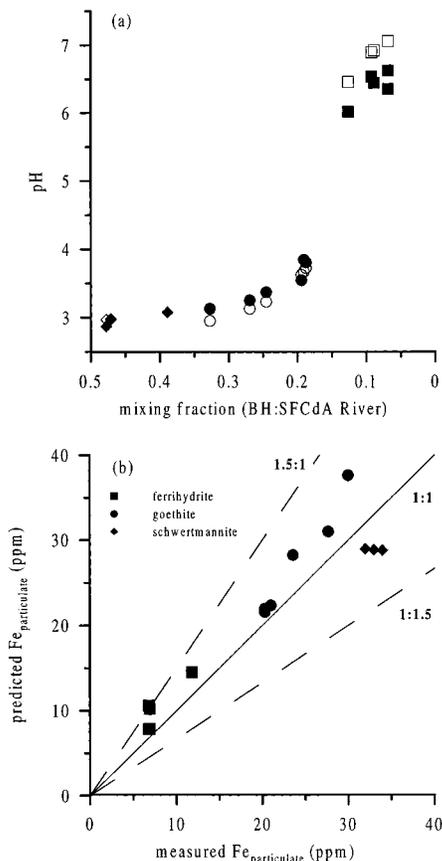
FIGURE 1. Predicted (open symbols) and observed (closed symbols) pH as a function of mixing fraction Bunker Hill (BH) effluent:South Fork Coeur d'Alene (SFCdA) River water (a). Predicted vs measured particulate Fe (b). Model predictions shown are those using the major iron oxide phase determined by X-ray diffraction. Dashed lines show errors of 1:1.5 and 1.5:1 (b).

the use of the equilibrium iron oxide phase matched to the XRD as a consistent modeling approach.

The formation of particulate Al in the mixing experiments at mixing fractions ≤0.13 is consistent with the amorphous material found by XRD analysis of these mixed solutions. Measured and predicted values were in good agreement at all mixing fractions using gibbsite as the equilibrium aluminum oxide phase. The formation of gibbsite is consistent with solubility diagrams for the solution conditions considered (28), and predicted and measured particulate Al agreed within a factor of 1.5. The results of the kinetic experiments indicated that there was no significant change in the particulate metal concentrations after 2 h. Notably, sorption onto manganese oxide phases was not considered because dissolved Mn was conservative throughout the mixing fraction range. Measured particulate Fe concentrations in the mixing experiments were greater than the corresponding measured POC values by factors ≥10; therefore, POC was not considered as a significant sorbing phase. Pb, Cu, As, Mo, and Sb exhibited nonconservative behavior or were removed from solution. For these metals, we assumed that the difference between measured total acid-soluble and dissolved metal values represents metals partitioned onto the iron and aluminum oxide phases via sorption processes. Zn removal was not considered because differences between large measured total acid-soluble and dissolved Zn concentrations were much smaller than the measurement errors.

Metal Partitioning in Mine Drainage Systems. Particulate Fe and Al values predicted using solution measurements, mineralogical data, and equilibrium speciation model were

in good agreement with measured values. XRD data characterizing the precipitates formed in the mixing experiments were used along with the diffuse double-layer SCM and surface complexation reactions for iron and aluminum oxide phases to compare observed with predicted metal partitioning.

Databases are available for HFO (9) and goethite (10) but not for schwertmannite or gibbsite. Metal sorption data for synthetic schwertmannite and a poorly ordered, goethite-bearing iron(III) oxyhydroxy sulfate precipitated in an acid mine drainage (AMD) system in New Zealand (29) were digitized using the computer software program Didger and modeled using MINTEQA2 (25) and HFO parameters for the iron oxide phases. Model simulations reproduced sorption of Pb, Cu, Zn, and Cd onto synthetic schwertmannite very well, and we concluded that HFO parameters are suitable for modeling metal partitioning on schwertmannite. Surface complexation constants for ion sorption on goethite (10) were included in the thermodynamic database; however, partitioning of Pb, Cu, As, Mo, and Sb were greatly underestimated using a goethite sorption model. Particulate Fe values predicted using goethite as the equilibrium solid phase were in good agreement with the measured values; therefore, we hypothesized that the surface formed in situ was not accurately characterized by the published surface parameters for goethite. In the goethite compilation, only one site type was used to model experimental sorption data. A comparison of surface complexation constants showed that log K values for goethite and weak log K values for HFO are similar, suggesting that the surface behavior of all iron oxide phases can be described with the same parameters (10). For low sorbate to sorbent ratios characteristic of the solutions considered, the "weak" goethite constants may not be sufficient, or strong sorption reactions such as those defined for HFO (9) may be necessary to accurately predict metal sorption. In addition, although the presence of crystalline iron oxide phases was ascertained by XRD analysis, the fractions crystalline and amorphous iron oxide solid material are impossible to determine.

On the basis of these observations, we chose to use a single set of model parameters and surface complexation constants (the HFO data) to simulate metal partitioning on schwertmannite, goethite, and amorphous iron oxide. Because surface complexation constants determined using the diffuse double-layer SCM are available only for Al$_2$O$_3$ (11), a single set of model parameters was similarly used to predict metal sorption on gibbsite. First, moles of observed particulate Pb, Cu, As, Mo, and Sb were normalized to moles of particulate Fe and plotted as a function of the mixing fraction (Figure 2a−e). Using the mineralogical data and PHREEQC to determine the moles of iron oxide formed at equilibrium, a single set of surface parameters for the iron oxides was used to predict metal sorption, shown by the dashed line. Model predictions using HFO or goethite for the formation of the iron oxide phase and mixing fractions = 0.14 or ≥0.145, respectively, were used to fill the gaps in the field data. Total sorption was calculated by dividing the sum of the predicted concentrations of the surface species formed at the strong and weak iron oxide surface sites by the moles of the iron oxide equilibrium phase. Model simulations indicated that sorption of metals on gibbsite was insignificant (approximately ≤1% of the total sorption).

Model predictions are in good agreement with measured values for Pb and Cu. Observed particulate Pb values are greater than the predictions of the sorption model at mixing fractions ≥0.18. These data suggest that, at the lower pH values associated with these mixing fractions (measured pH ≤ 3.8), some Pb may be associated with a phase other than HFO. A study comparing model predictions with measured Pb concentrations in AMD from the Pecos Mine, NM, suggests
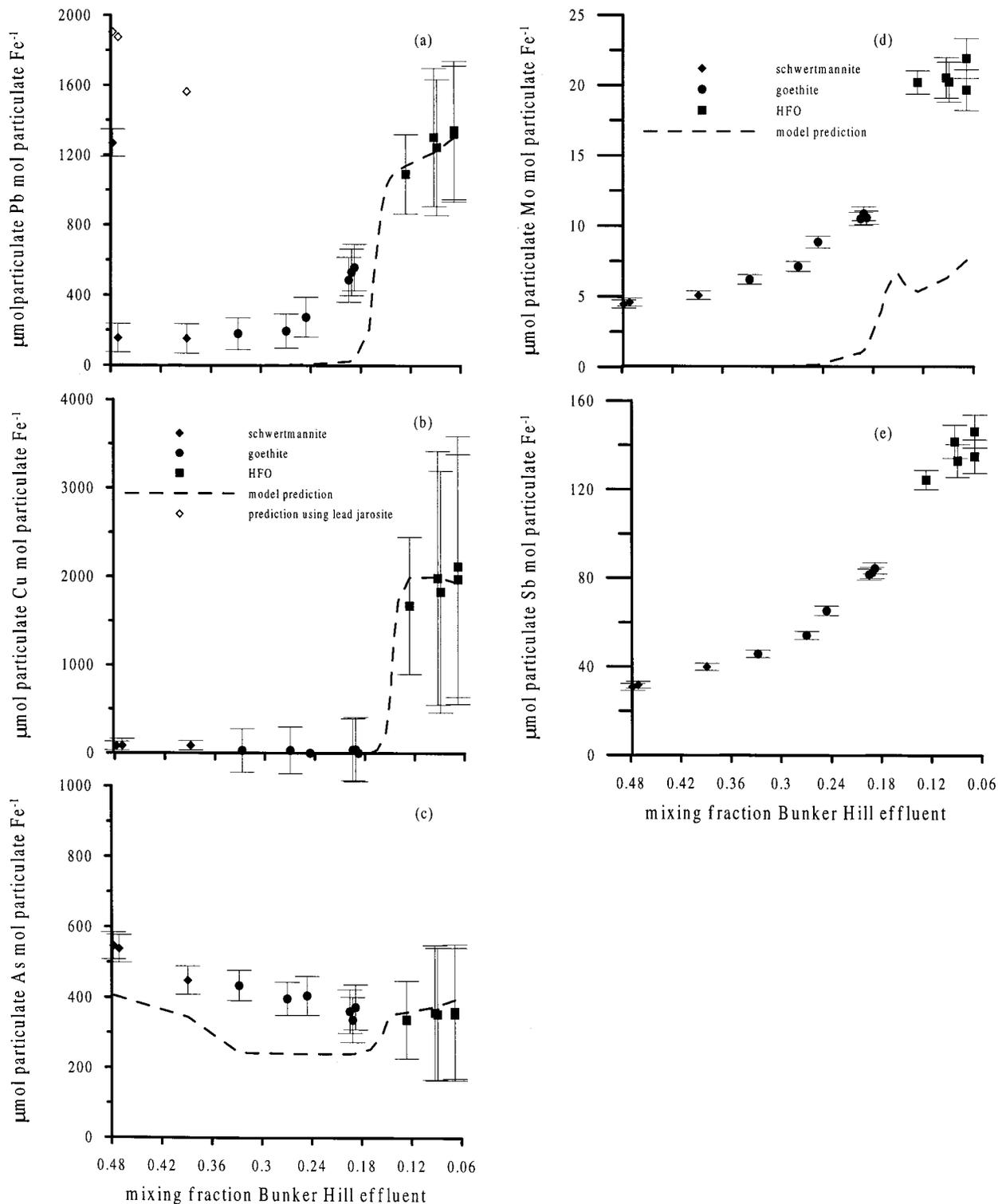
FIGURE 2. Measured ratios of particulate Pb (a), Cu (b), As (c), Mo (d), and Sb (e) to particulate Fe, along with model simulations, are plotted as a function of mixing fraction Bunker Hill effluent. The major composition of the iron oxide phases determined by XRD analysis is shown using the symbols diamond (schwertmannite), circle (goethite), and square (amorphous material). The dashed line shows predicted metal partitioning using a sorption model and a single set of model parameters for the iron oxides. Predicted partitioning of Pb, including precipitation of lead jarosite, is shown by the open diamonds.

that Pb is removed primarily by precipitation of cerussite ($PbCO_3$) (15). iron oxide concentrations were relatively low in the NM mine drainage system, however, and sorption processes did not contribute significantly to metal removal. Initial equilibrium calculations for our solution conditions did not indicate supersaturation of any Pb-containing mineral, including cerussite or anglesite ($PbSO_4$). Saturation

indices calculated by Chapman et al. (2) in their investigation of an acidic drainage stream contaminated by mine adits and spoil heaps in Lithgow, NSW, indicated that lead jarosite, $PbFe_6(SO_4)_4(OH)_{12}$, was supersaturated over the entire stream reach, and X-ray powder diffraction analysis of the stream sediment indicated the presence of crystalline jarosites. Lead jarosite was added to the PHREEQC database a posteriori
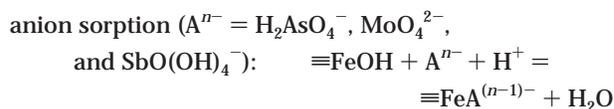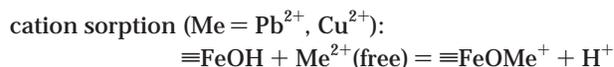
and investigated as a possible mechanism for the formation of particulate Pb. Initial model simulations without equilibration of any solid phase indicated supersaturation of lead jarosite at all mixing fractions. However, the final model analyses including precipitation of the pure iron oxide phases indicated that lead jarosite forms only with schwertmannite as the equilibrium iron oxide phase or at mixing fractions ≥ 0.38. A simple sorption model is reasonable for the pH range where Pb has a strong affinity for the iron oxide surfaces; but at pH values below the sorption edge of the metal of interest, precipitated phases may make a significant contribution to metal partitioning. Particulate Pb values determined from the ratios of moles lead jarosite to the total moles of precipitated Fe are shown in addition to values calculated with the simple sorption model in Figure 2a. TEM analyses of mineral grains collected in the CdA Mining District also indicate that Pb may be coprecipitated with iron oxides (*30*). However, using the proposed Fe:Pb stoichiometry from this study, calculated values account for only $\approx 5\%$ of the measured particulate Pb values from the mixing experiments. It is interesting to note that the data point at mixing fraction 0.48 is still underpredicted by the equilibrium precipitation model. Although measured values of particulate Cu at mixing fractions ≥ 0.19 are not significant relative to the calculated error, the position of the predicted Cu sorption edge is in reasonable agreement with the observed data.

Model predictions for As sorption are in good agreement with measured values at mixing fractions ≤ 0.12 or at higher pH values (measured pH ≥ 6.0). In initial mixing models with no precipitation of solid phases, $Ba_3(AsO_4)_2$ was predicted to be supersaturated. However, precipitated As was negligible in the final models including all equilibrium phases, in agreement with the observed conservative behavior of Ba. At mixing fractions ≥ 0.19 (measured pH ≤ 3.1), As sorption is underpredicted by the goethite and schwertmannite models. The difference between measured and modeled values is greater than can be accounted for by the calculated variability in the particulate As and Fe measurements, and measured versus modeled pH values are within ± 0.1 log unit at pH ≤ 3.1. As may substitute for up to 3% Fe mol mol^{-1} in crystalline iron oxides (*30*); however, this substitution would not account for the degree of respective under- and overprediction of particulate As and Fe at high mixing fractions. Particulate Mo and Sb values were greatly underpredicted by the model across the pH range. The sawtooth in the prediction of particulate Mo to particulate Fe at mixing fraction $\cong 0.15$ results from the slight discontinuity in predicted pH and particulate Fe that occurs when switching from the ferrihydrite to goethite model. Shokes and Möller (*31*), who studied metal removal from acid rock drainage collected from the Berkeley Pit, MT, also observed significant removal of dissolved Sb upon treatment of the drainage water with colloidal Fe. These observations suggest that there may be a removal mechanism for As, Mo, and Sb that is not represented by the model. Although the data indicated that POC was not present in concentrations significant for consideration as a sorbing phase, its presence and the presence of other ill-defined solution and solid-phase organic ligands could influence metal partitioning. The roles of various forms of natural organic matter in the distribution of contaminants in the environment have been studied (e.g., refs *32*–*34*), and applications involving surface complexation modeling remain an important area for continued development. Additionally, log K values for Mo and Sb surface reactions were determined from linear free energy relationships rather than experimental data, and this may introduce further limitations for modeling complex natural systems. Without a totally comprehensive set of both surface complexation constants and solution measurements, it is difficult to assess whether discrepancies between model and mea-

sured results are more likely a result of errors in the assumptions of the model, or a result of gaps in the measured or thermodynamic data.

Second, the partitioning of metals in both the mixing experiments and observed in solutions collected from adits and tailings piles in September 1996 and June 1997 was compared to model results (Figure 3). Methods of sample collection and analysis were as described in ref *17*. To be consistent with the mechanism of cation sorption assumed in the diffuse double-layer SCM, we assumed that Pb and Cu partitioned in the solid phase was a result of sorption of the free metal ion on the iron oxide surface. Metal oxyanion speciation over a wide pH range can be more complex, with more than one surface reaction often required to model experimental data (*9*). We chose to represent As, Mo, and Sb partitioning by the sorption of $H_2AsO_4^-$, MoO_4^{2-}, and $SbO(OH)_4^-$, respectively.

The following equations were linearized:

cation sorption (Me = Pb^{2+}, Cu^{2+}):
$$\equiv FeOH + Me^{2+}(free) = \equiv FeOMe^+ + H^+$$

anion sorption ($A^{n-} = H_2AsO_4^-$, MoO_4^{2-},
and $SbO(OH)_4^-$):
$$\equiv FeOH + A^{n-} + H^+ = \equiv FeA^{(n-1)-} + H_2O$$

and the resulting terms were plotted as a function of pH:

cation partitioning:
$$\log\left(\frac{[FeOMe^+]}{[FeOH][Me^{2+}(free)]}\right)$$

anion partitioning:
$$\log\left(\frac{[FeOH][A^{n-}]}{[FeA^{(n-1)-}]}\right)$$

Model fits were determined using the predicted solution concentrations of Pb^{2+}(free), Cu^{2+}(free), $H_2AsO_4^-$, MoO_4^{2-}, and $SbO(OH)_4^-$ in the mixing experiments. Measured total dissolved metal concentrations for each mixing experiment and for each adit and tailings pile drainage solution were input into PHREEQC and MINTEQA2, respectively, to estimate measured Pb^{2+}(free), Cu^{2+}(free), $H_2AsO_4^-$, MoO_4^{2-}, and $SbO(OH)_4^-$ concentrations.

Assuming that particulate Fe sampled in the CdA Mining District in 1996 and 1997 has the same surface characteristics as the newly formed iron oxide phases from the mixing experiments, we expected the data to fall on a straight line when both sets of data were plotted. The slope of the line represents moles of H^+ generated or taken up per mole of cation or metal oxyanion sorbed, respectively. Plots generated for Pb, Cu, As, Mo, and Sb are shown in Figure 3a–e. Assuming that the absolute errors for dissolved measurements of Pb, Cu, As, Mo, and Sb are equal to those calculated for the particulate measurements, we illustrate the total propagated error for Cu, As, Mo, and Sb in Figure 3b–e. Error bars for Pb at mixing fractions ≥ 0.33 are shorter than the symbol height and at mixing fractions ≤ 0.12 are large ($\geq \pm 13$) and not shown. Measured and predicted dissolved Pb concentrations are in good agreement, and the accuracy of the dissolved measurements is good. However, using this approach, the calculated relative error in the dissolved Pb measurement is large at the higher pH values.

Data for Pb and Cu appear to be generally linear, with a slope $\cong 1$. A comparison of the y-intercept values of the Pb and Cu plots suggests that the overall relative sorption affinity for the particulate Fe is Cu < Pb. In the solutions studied, $PbCO_3^-$ is the dominant Pb species at higher pH values (mixing fractions ≤ 0.12 and measured pH values ≥ 6.0), and
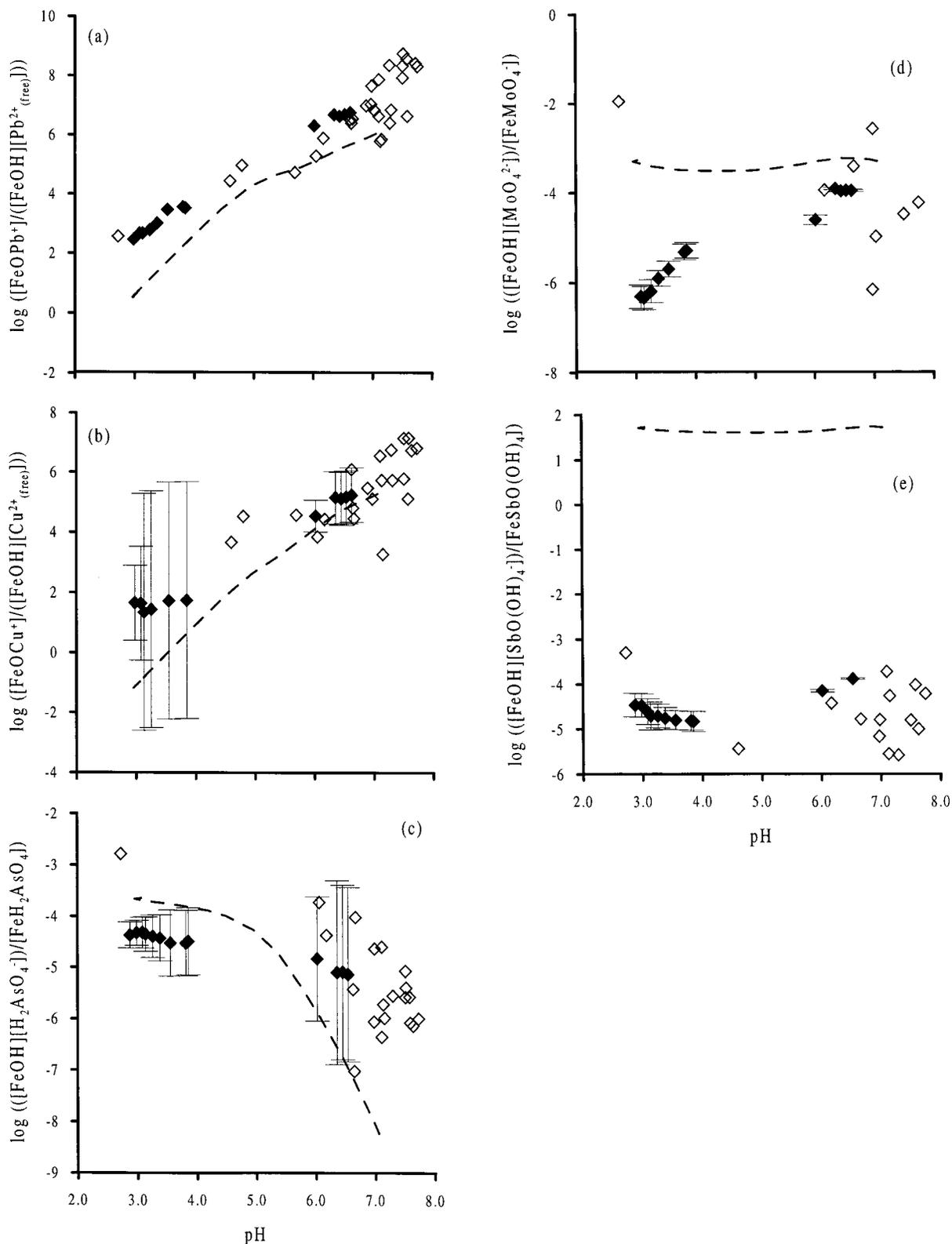
FIGURE 3. Metal partitioning as a function of pH is plotted using sorption reactions for Pb (a), Cu (b), As(V) (c), Mo (d), and Sb(V) (e). Data from the mixing experiments performed in 1999 with Bunker Hill effluent and South Fork Coeur d'Alene River water are shown by the closed diamonds, and data collected from the Coeur d'Alene Mining District in 1996 and 1997 are shown by the open diamonds. PHREEQC model predictions for the mixing experiments are shown by the dashed line.

differences between total dissolved Pb and Pb^{2+}(free) concentrations are pronounced in this pH range. Assuming the sorption mechanism described above, we attempted to minimize errors in our comparisons by using Me^{2+}(free) in all calculations. Figure 2a illustrates that the model under-

estimates the observed particulate Pb:Fe ratios at low pH values, which is consistent with the discrepancy between the measured data and model predictions shown in Figure 3a. For particulate As, Mo, and Sb, we expect the measured data to fall on a straight line with a slope of approximately

−1 assuming sorption of $H_2AsO_4^-$, MoO_4^{2-}, and $SbO(OH)_4^-$. The reaction models chosen for As, Mo, and Sb are reasonable for the pH range studied, but metal oxyanion partitioning appears to be generally less well-predicted using the sorption approach with the goodness of fit decreasing: As > Mo > Sb. The reaction model appears most reasonable for As (Figure 3c) considering error estimates, but the As data from the mixing experiments have a slope $\cong -1/4$. Shown in Figure 2d,e, particulate Mo and Sb are poorly predicted by the sorption model, reflected also in Figure 3d,e. In addition, the slopes of the Mo and Sb data are ≥ 0. These results provide further evidence that As, Mo, and Sb sequestered in the newly formed particulate fractions in the mixing experiments may not be well-described by the sorption model. In general, data collected from the CdA Mining District in 1996 and 1997 have more scatter than the mixing experiments, further suggesting that there may be current limitations to predicting metal partitioning over a wide range of solution compositions and sorbing solid phases.

We have combined field, laboratory, and modeling studies to evaluate the application of an empirical speciation and sorption model to predicting metal partitioning in a complex natural system. The sorption model, with a single set of surface parameters and surface complexation constants derived from simple laboratory systems, predicts well the partitioning of Pb, Cu, and As on (i) newly formed iron oxides precipitated from the mixing of an acidic, metals-laden effluent with neutral SFCdA River water and (ii) particulate Fe sampled in the CdA Mining District from sites with widely varying pH and dissolved metal concentrations. Published HFO surface parameters were shown to be universal in their application to modeling metal sorption on both amorphous and crystalline equilibrium iron oxide phases, including schwertmannite. However, the use of this simple model to simulate a complex geochemical environment did not work for all metals. There may be additional removal mechanisms for As, Mo, and Sb that are not represented by the model, and a more complex model may be necessary.

Agreement between empirical model predictions and field data does not verify implicitly the selected model parameters, but allows us to evaluate the surface complexation model and its application. The molecular nature of surface complexes or surface parameters for natural particles may vary widely and may be unknown. An alternate modeling approach would newly evaluate experimental data using different surface parameters and/or reaction stoichiometries. This approach, while valid, would deviate from the consistent method previously set forth and would require the additional tasks of optimizing the experimental data and physically characterizing the solid phases. Moreover, it would be unclear which model parameters would be suitable for which situations. Additional data, including data from spectroscopic studies of natural particulates, laboratory studies of metal sorption on both natural and well-characterized synthetic solid phases, and data describing metal−organic interactions, are needed to bring us closer to the goal of a totally comprehensive set of equilibrium solution and surface complexation constants for a given SCM. Our results demonstrate the current ability to use equilibrium speciation models along with measured data and universal model parameters to predict trace metal partitioning in contaminated areas.

Acknowledgments

Literature Cited

(1) Plumlee, G. S.; Nash, J. T. In *Preliminary Compilation of Descriptive Geoenvironmental Mineral Deposit Model*; duBray, E. A., Ed.; U.S. Geological Survey: Reston, VA, 1995; pp 1−9.

(2) Chapman, B. M.; Jones, D. R.; Jung, R. F. *Geochim. Cosmochim. Acta* **1983**, *47*, 1957−1973.

(3) Hudson-Edwards, K. A.; Macklin, M. G.; Curtis, C. D.; Vaughan, D. J. *Environ. Sci. Technol.* **1996**, *30*, 72−80.

(4) O'Day, P. A.; Carroll, S. A.; Waychunas, G. A. *Environ. Sci. Technol.* **1998**, *32*, 943−955.

(5) Carroll, S. A.; O'Day, P. A.; Piechowski, M. *Environ. Sci. Technol.* **1998**, *32*, 2, 956−965.

(6) Johnson, C. A. *Geochim. Cosmochim. Acta* **1986**, *50*, 2433−2438.

(7) Ranville, J. F.; Smith, K. S.; Macalady, D. L.; Rees, T. F. In *U.S. Geological Survery Toxic Substances Hydrology Program−Proceedings of the Technical Meeting, Phoenix, Arizona, September 26−30, 1988;* U.S. Geological Survey Water-Resources Investigations Report 88-4220; U.S. Geological Survey: Reston, VA, 1989.

(8) Stollenwerk, K. *Appl. Geochem.* **1994**, *9*, 353−369.

(9) Dzombak, D. A.; Morel, F. M. M. *Surface Complexation Modeling: Hydrous Ferric Oxide*; John Wiley & Sons: New York, 1990.

(10) Mathur, S. M. Development of a Database for Ion Sorption on Goethite Using Surface Complexation Modeling. M.S. Thesis, Carnegie Mellon University, Pittsburgh, PA, 1995.

(11) Paulson, A. J. *Fate of Metals in Surface Waters of the Coeur d' Alene Basin, Idaho*; United States Department of the Interior Bureau of Mines Report of Investigations 9620; U.S. Government Printing Office: Washington, DC, 1996.

(12) Davis, A.; Runnells, D. D. *Appl. Geochem.* **1987**, *2*, 231−241.

(13) Smith, K. S.; Ranville, J. F.; Plumlee, G. S.; Macalady, D. L. In *Adsorption of Metals by Geomedia: Variables, Mechanisms, and Model Applications*; Jenne, E. A., Ed.; Academic Press: San Diego, CA, 1998; pp 521−547.

(14) Schemel, L. E.; Kimball, B. A.; Bencala, K. E. *Appl. Geochem.* **2000**, *15*, 1003−1018.

(15) Berger, A. C.; Bethke, C. M.; Krumhansl, J. L. *Appl. Geochem.* **2000**, *15*, 655−666.

(16) Paulson, A. J.; Balistrieri, L. S. *Environ. Sci. Technol.* **1999**, *33*, 3850−3856.

(17) Balistrieri, L. S.; Bookstrom, A. A.; Box, S. E.; Ikramuddin, M. *The Geochemistry of Water Draining from Adits and Tailings Piles in the Coeur d' Alene Mining District*; U.S. Geological Survey Open File Report 98-127; U.S. Department of the Interior: Washington, DC, 1998.

(18) Jambor, J. L. In *Short Course Handbook Volume 22 on Environmental Chemistry of Sulfide Mine-Wastes*; Jambor, J. L., Blowes, D. W., Eds.; Mineralogical Association of Canada: Waterloo, ON, 1994; pp 59−102.

(19) Horowitz, A. J.; Elrick, K. A.; Cook, R. B. *Hydrol. Processes* **1993**, *7*, 403−423.

(20) Horowitz, A. J.; Elrick, K. A.; Robbins, J. A.; Cook, R. B. *Hydrol. Processes* **1995**, *9*, 35−54.

(21) Daniels, S. H. Fledgling Remediation Firm Stakes Claim at Bunker Hill. *Eng. News-Record* **1997**.

(22) Mitchell, P.; Wheaton, A. *Mining Environmental Management*; Technical Paper; 1999.

(23) Stumm, W.; Morgan, J. J. *Aquatic Chemistry*, 3rd ed.; John Wiley & Sons: New York, 1996.

(24) Parkhurst, D. L.; Appelo, C. A. J. *User's Guide to PHREEQC (Version 2). A Computer Program for Speciation, Batch-Reaction, One-Dimensional Transport, and Inverse Geochemical Calculations*; 2000.

(25) Allison, J. D.; Brown, D. S.; Novo-Gradac, K. J. *MINTEQA2/PRODEFA2. A Geochemical Assessmnet Model for Environmental Systems: Version 3.0 User's Manual*; U.S. Environmental Protection Agency: Athens, GA, 1991.

(26) Turner, D. R.; Whitfield, M.; Dickson, A. G. *Geochim. Cosmochim. Acta* **1981**, *45* 855−881.

(27) Bigham, J. M.; Schwertmann, U.; Traina, S. J.; Winland, R. L.; Wolf, M. *Geochim. Cosmochim. Acta* **1996**, *60* 2111−2121.

(28) Nordstrom, D. K. *Geochim. Cosmochim. Acta* **1982**, *46*, 681−692.

(29) Webster, J. G.; Swedlund, P. J.; Webster, K. S. *Environ. Sci. Technol.* **1998**, *32*, 1361−1368.

(30) Hooper, R. L. University of Wisconsin−Eau Claire (unpublished).

(31) Shokes, T. E.; Möller, G. *Environ. Sci. Technol.* **1999**, *33*, 282−287.

(32) Davis, J. A. *Geochim. Cosmochim. Acta* **1984**, *48*, 679−691.

(33) Xue, H.; Stumm, W.; Sigg, L *Water Res.* **1988**, *22*, 917−926.

(34) Santschi, P. H.; Lenhart, J. J.; Honeyman, B. D. *Mar. Chem.* **1997**, *58*, 99−125.